



Nyffeler et al.:

Design of a High-Throughput Human Neural Crest Cell Migration Assay to Indicate Potential Developmental Toxicants

Supplementary Data

Tab. S1: List of antibodies used in this study

Target name	Antibody name	Host	Dilution	Catalog #	Provider
HNK1	Monoclonal anti-human CD57/HNK-1	mouse IgM	1:200	C6680	Sigma
p75	NGFr (ME20.4, p75) Mouse Monoclonal	mouse IgG1	1:200	#AB-N07	Advanced Targeting Systems
Nestin	Monoclonal Mouse IgG1 clone #196908	mouse IgG1	1:500	MAB1259	R&D Systems
Pax6	Purified anti-Pax-6 antibody	rabbit	1:200	PRB-278P	Covance
GFAP	Anti-GFAP antibody [2A5]	mouse IgG1	1:1000	ab4648	Abcam
F-actin	Alexa Fluor® 568 Phalloidin	–	1:1000	A12380	Invitrogen

Tab. S2: List of primers used in this study for quantitative RT-PCR

Gene	Accession No.	Designation	Primer Sequences from 5' to 3' end	Fragment length
CDH1	NM_004360.3	CDH1_F	GCT ACA CGT TCA CGG TGC CC	211 bp
		CDH1_R	GTG GAG TCC CAG GCG TAG AC	
CDH2	NM_001792.3	CDH2_2F	GGC GTC TGT AGA GGC TTC TG	211 bp
		CDH2_2R	CAC GGC ATA CAC CAT GCC ATC	
CDH4	NM_001794.3	CDH4_F	ATC AAC GTG CCC GAG AAC TC	219 bp
		CDH4_R	GTG GGC TCG GAG GTG GTA AG	
CDH6	NM_004932.3	CDH6_F	AGA AAA GGG CCC TGG AGC TC	198 bp
		CDH6_R	GAT CTC CTG CTC CAT CTC CTG	
CDH7	NM_033646.1	CDH7_F	AGC AGG CCT ACT ACA CGC TC	194 bp
		CDH7_R	CGT CGC TGT CAC TTG TAC CAC	
CDH8	NM_001796.4	CDH8_F	GGA GGC TTG ACA TTC GCC AG	184 bp
		CDH8_R	TCT CCG GTC TGC AGC CAT CC	
CDH9	NM_016279.3	CDH9_F	ACG GTA AAA TGC TAC GTC GC	173 bp
		CDH9_R	AAA TAG ACT GCC AGC CCC ATC	



This is an Open Access article distributed under the terms of the Creative Commons Attribution 4.0 International license (<http://creativecommons.org/licenses/by/4.0/>), which permits unrestricted use, distribution and reproduction in any medium, provided the original work is appropriately cited.

<https://doi.org/10.14573/altex.1605031s>



Gene	Accession No.	Designation	Primer Sequences from 5' to 3' end	Fragment length
CDH10	NM_006727.3	CDH10_2F	TCT GAG GCC AGT AGA GCC AG	213 bp
		CDH10_2R	GGC TGC CCT TGA AGT ATG CTG	
CDH11	NM_001797.2	CDH11_F	GCC TGA CCC CGT GCT TGT GG	198 bp
		CDH11_R	TCC CTG TCC ACC GCC TGA GC	
CDH18	NM_004934.3	CDH18_F	CTA TGG AAA CAG CGC TCG GG	174 bp
		CDH18_R	AGC CCT CCA ACT TGC CCA GC	
CDH19	NM_021153.2	CDH19_F	ACT GGA AGG GCT GTG GAA CC	214 bp
		CDH19_R	GCT GGC CTT GAA GTA AGC TG	
CDH20	NM_031891.2	CDH20_F	AGC ATT CTT CAG GGC CAG CC	214bp
		CDH20_R	TCT GGG GAA AGC GGG GTG GG	
ITGa1	NM_181501.1	ITGA1_F	CTG CTG GCT CCT CAC TGT TG	173 bp
		ITGA1_R	TGG GTT GGC CAA CTA ACG GAG	
ITGa2	NM_002203.3	ITGA2_2F	GTT TGG CTA TGC AGT GCA GC	211 bp
		ITGA2_2R	CAA GCC GAG GCT CAT GTT GG	
ITGa3	NM_002204.2	ITGA3_2F	GCC CCA CGC CTG ATG CTC TG	195 bp
		ITGA3_2R	GGG GGC ACC AGC CAG GAG C	
ITGa4	NM_000885.4	ITGA4_F	GGGCAAGGAAGTTCCAGGTTACATTG	196 bp
		ITGA4_R	GTCCCGCACATCTTTCCGCATAAATG	
ITGa5	NM_002205.2	ITGA5_2F	CCA GCC CCA CAC AGT GCA CC	198 bp
		ITGA5_2R	GTG GCT CCT TCT CTG TGC GC	
ITGa6	NM_001079818.1	ITGA6_F	CGG CGC AGC CTT CAA CTT GG	201 bp
		ITGA6_R	TCG CAG CTG TAC AGC CCT CC	
		ITGA6_2F	CGA GGA CAA GCG GCT GTT GC	197 bp
		ITGA6_2R	GGC TCT GGA CGG TGA CCC CC	
ITGa7	NM_001144996.1	ITGA7_F	AGA CGC CAT GTT CCA GCT CC	198 bp
		ITGA7_R	CCA CAG CCT TGC TTC AGG AAG	
ITGa8	NM_003638.1	ITGA8_F	TGC AGG CAG ATA CCG TTT GAC	199 bp
		ITGA8_R	AGC AGG TGC CAA CTG GGT CC	
ITGa9	NM_002207.2	ITGA9_F	CGG CTA CGC AGT TCT GGA GC	200 bp
		ITGA9_R	TCT TTC CGC AGG ACG TGC CC	
ITGa10	NM_003637.3	ITGA10_2F	TCA GGC ATG GAA CTC CCC TTC	205 bp
		ITGA10_2R	CTG AAG GCC CAT CCC AGG GG	
ITGa11	NM_001004439.1	ITGA11_2F	CCA GGA CCG CCT TCT TTG GC	204 bp
		ITGA11_2R	CGC ATG TTG TCT TTC CGC TC	
ITGallb	NM_000419.3	ITGA2B_F	GGA CCT TGT GCT GCC CCT CC	204 bp
		ITGA2B_R	CCA GGG GCA CAG GAA CAC GC	
ITGAV	NM_002210.4	ITGAV_F	TGG TCT TCT ACC CGC CGG TG	197 bp
		ITGAV_R	CCA ACA GGC TCT CGC TCC TG	



Gene	Accession No.	Designation	Primer Sequences from 5' to 3' end	Fragment length
ITGb1	NM_000211.3	ITGB1_F	CAC CAG CTA AGC TCA GGA ACC C	204 bp
		ITGB1_R	AGC CAA TCA GTG ATC CAC AAA CTG C	
ITGb2	NM_000211.3	ITGB2_F	TCG GGT GCG TCC TCT CTC A	199 bp
		ITGB2_R	CTT GTG GGG TCC ATG ATG TCG TC	
		ITGB2_2F	TGC GTC CTC TCT CAG GAG TG	199 bp
		ITGB2_2R	CGA GGC TTG TGG GGT CCA TG	
ITGb3	NM_000212.2	ITGB3_F	CCC CTG CTA TGA TAT GAA GAC CAC CT	173 bp
		ITGB3_R	CAC AGA CTG TAG CCT GCA TGA TGG	
ITGb5	NM_002213.3	ITGB5_F	CTG TAC GCC TGC CTC CTG G	182 bp
		ITGB5_R	GCC CTC AGA TCA CAC CGA GAG	
ITGb6	NM_000888.3	ITGB6_F	TCA GTG TGC CTG GTG TGC TC	210 bp
		ITGB6_R	AAG CTT TGA GGC GCA ATC TG	
ITGb8	NM_002214.2	ITGB8_F	TGC GCT GGG TCC AGA ATG TG	212 bp
		ITGB8_R	CTG GAC GCA GCT GGA TAG AC	
GAPDH	NM_002046.5	GAPDH_2F	ATG GAG AAG GCT GGG GCT CA	234 bp
		GAPDH_2R	AGT GAT GGC ATG GAC TGT GGT CAT	

Differentiation of NCC from iPSC

The differentiation of NCCs from iPS (IMR90) cells was performed by dual SMAD inhibition instead of the MS5-induction step, following exactly our recently published protocol (Mica et al., 2013; Chambers et al., 2016). At day 11 of differentiation, cells were re-plated on poly-L-ornithine/fibronectin/laminin coated dishes and expanded and cryopreserved exactly as the hESC-derived NCC.

Alternatively, iPSC were generated from the human fibroblast line GM02036. Sendai virus was used as non-integrating vector to introduce the Yamanaka factors (Invitrogen) as described earlier (Choi et al., 2014). In these iPS (GM02036) cells, the silencing of ectopic genes (Yamanaka factors) was confirmed by PCR. Pluripotency was confirmed by measurement of protein expression of Nanog, Oct4, and SSEA3/4 at passage 12. Differentiation of NCCs from iPS (GM02036) cells was performed using the rosette induction protocol with a small modification: instead of N2S medium, Neurobasal medium supplemented with N2, B27 without vitamin A (both from Gibco), L-glutamine and EGF/FGF2 was used. The same medium composition was used for the cMINC assay using these cells.

Time-lapse video microscopy to assess cell proliferation and cell tracking

The time-lapse experiment was performed using an Axio Observer.Z1 microscope (Zeiss), equipped with an AxioCam MRm camera and a live-cell chamber (equilibrated at 37°C and

9% CO₂). Phase contrast images of the migration zone were acquired every 10 min using a 5x objective. Afterwards, cells were stained with calcein-AM and H-33342 and migration as well as viability were quantified exactly as described in “NCC migration setup” (manuscript main part) to ensure that the toxicants worked as under standard cMINC conditions with exposure in a standard incubator.

To assess cell proliferation in the migration zone, a circle of radius 1 mm was drawn manually by an experienced person on the time-lapse images to define the ROI. Cell divisions in this ROI were manually counted, supported by a Fiji (Schindelin et al., 2012) script provided by Martin Stöckl (Bioimaging Center of the University of Konstanz (BIC)). The experimenter was blind to the respective treatments. The number of counted cell divisions was normalized to the number of migrated cells in the same well as measured with the H-33342 and calcein staining. The time-lapse experiment was performed once with three technical replicates for untreated, CytoD and FBS and with two technical replicates for taxol, LiCl, CdCl₂ and AraC.

For cell tracking experiments, cell tracking was performed manually using the ImageJ plugin “Manual Tracking”. For each biological replicate, ten individual cells were traced per condition (and 20-30 cells for the untreated control). The cumulated distance of each cell was normalized to the median of the untreated control. Statistical significance was calculated on the combined data of three biological replicates using a Wilcoxon rank sum test to compare treatments to the untreated control.

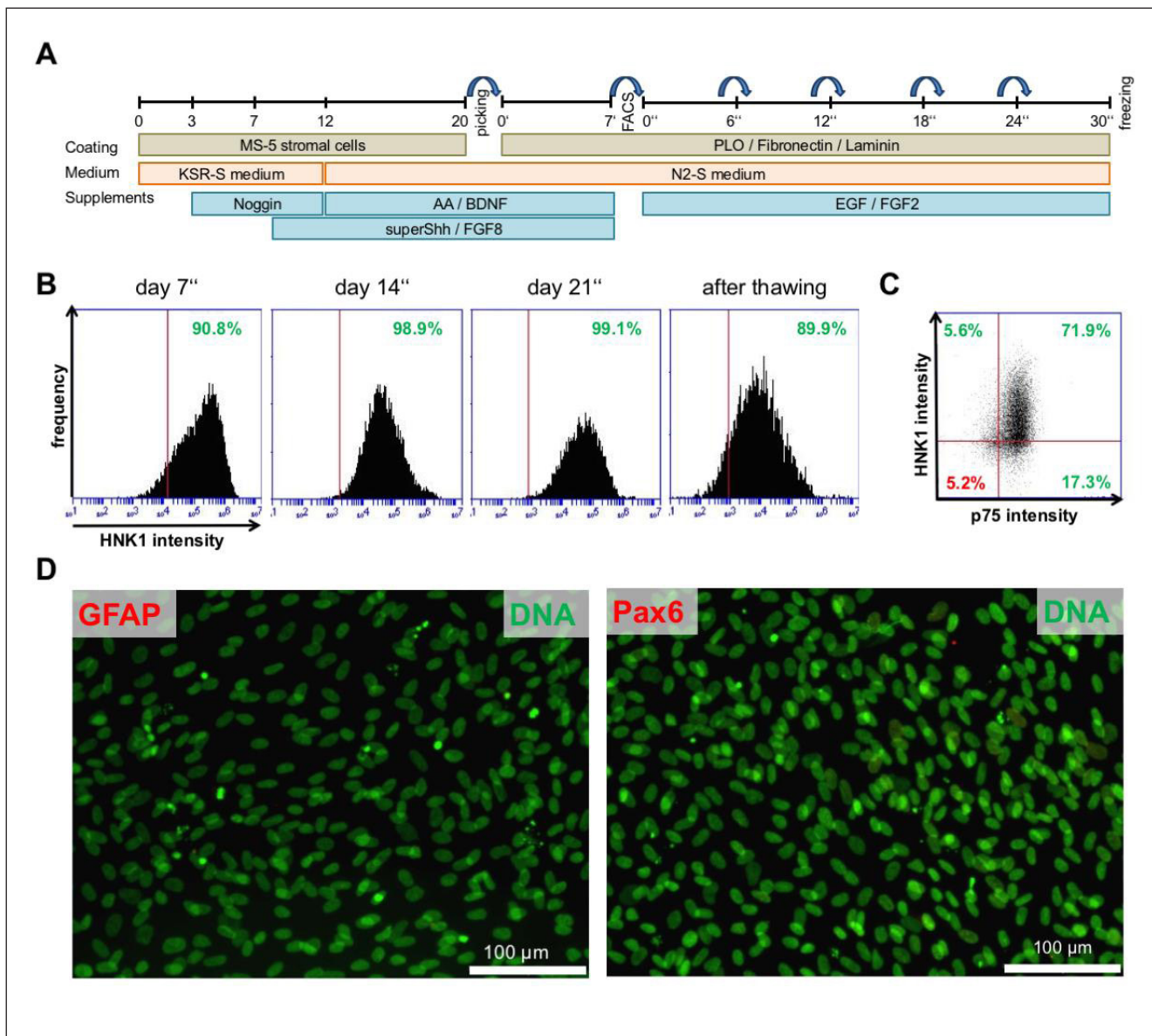


Fig. S1: Characterization of H9-derived NCCs

(A) Graphical representation of the differentiation procedure to obtain NCCs from human pluripotent stem cells. In a first step, cells were differentiated on MS-5 feeder cells for 20 days to a rosette stage. The rosettes were picked and differentiated further for seven days (day 0'-7'). Then, the target population was obtained by FACS sorting (HNK-1⁺/DII⁻ cells), and was further expanded for up to 30 days before freezing (days 0''-30''). (B) The expression of the NCC marker HNK-1 was monitored by FACS analysis during the expansion phase (days 7''-21''); similar data were also obtained after thawing of a frozen sample. (C) Representative 2D expression plot obtained by FACS analysis of cells after thawing: about 95% of all cells expressed either of the two NCC markers HNK-1/p75; 70-80% of the cells were double-positive. (D) NCCs were thawed and seeded under standard assay conditions. After 24 h, cells were fixed and stained for GFAP (left) and Pax6 (right). The scale bar corresponds to 100 μ m. Note that in the two images no positive cells are shown, as they were usually not evident under our culture conditions. Both antibodies were used in parallel on central neural precursor cells (Pax6) and astrocytes (GFAP), and they worked well under our staining conditions.

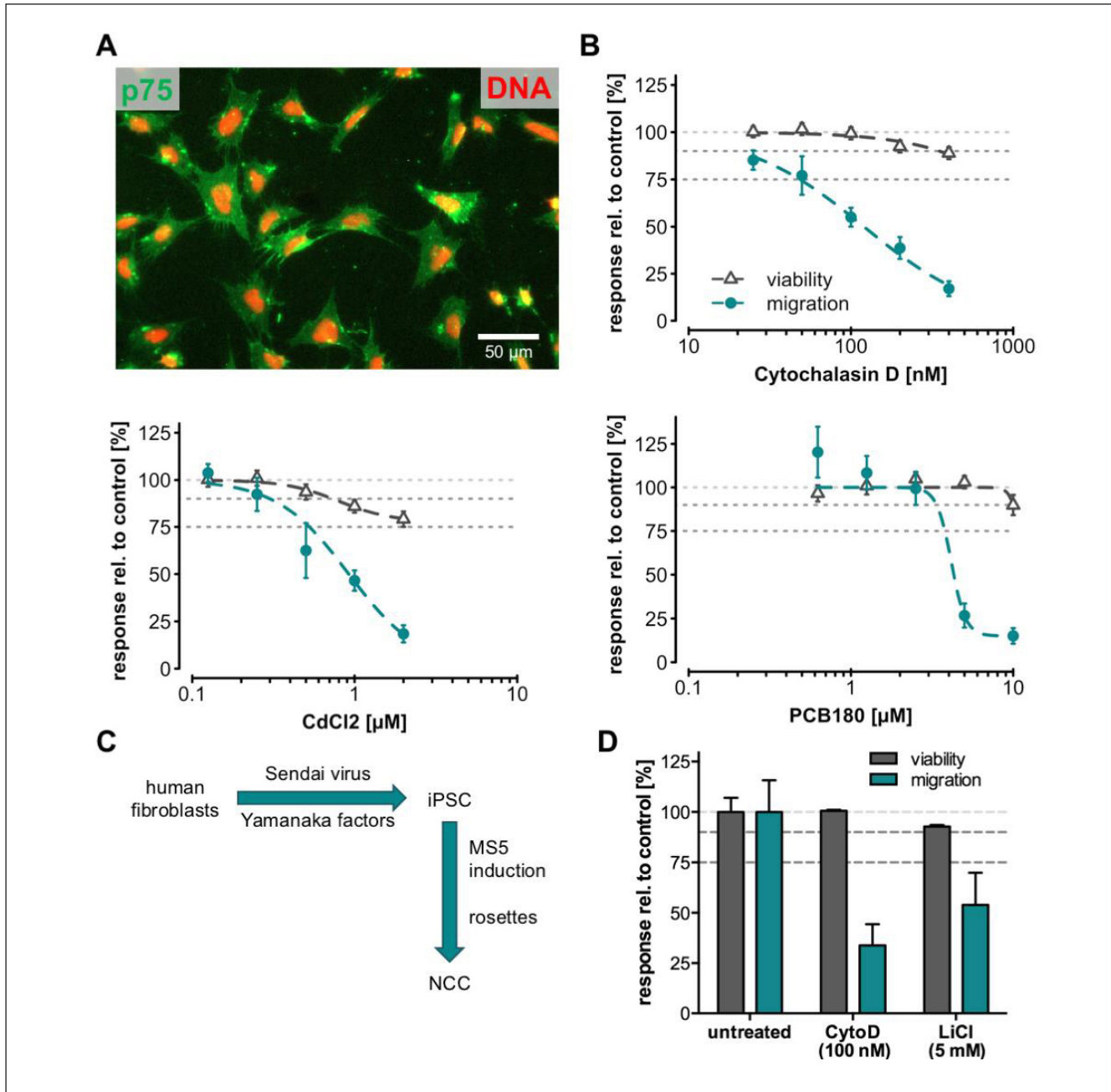


Fig. S2: Differentiation of iPSC into NCCs and use in the cMINC assay

(A) To obtain NCCs, iPS (IMR90) cells were differentiated via dual SMAD inhibition for 11 days towards Sox10 positive NCCs as described in Mica et al. (2013) and further expanded for two weeks in N2-S medium supplemented with EGF and FGF2 before freezing. After thawing, cells were seeded on glass for 24 h before they were fixed and labelled with immunofluorescent antibodies against p75 and counterstained by H-33342. The scale bar corresponds to 50 μm . (B) The cMINC assay was performed using these iPS (IMR90)-derived NCCs under optimized assay conditions (24 h toxicant exposure; see also Fig. 4). Concentration-response curves were obtained for three exemplary compounds. All values are normalized to untreated controls. Data are means \pm SD from three different experiments. (C) Graphical representation of the procedure to obtain NCCs from human fibroblasts via iPSC. (D) Preliminary data of iPS (GM02036)-derived NCC under optimized cMINC assay conditions (as in B). All values are normalized to untreated controls. Data are means \pm SD of 4 technical replicates from one experiment.

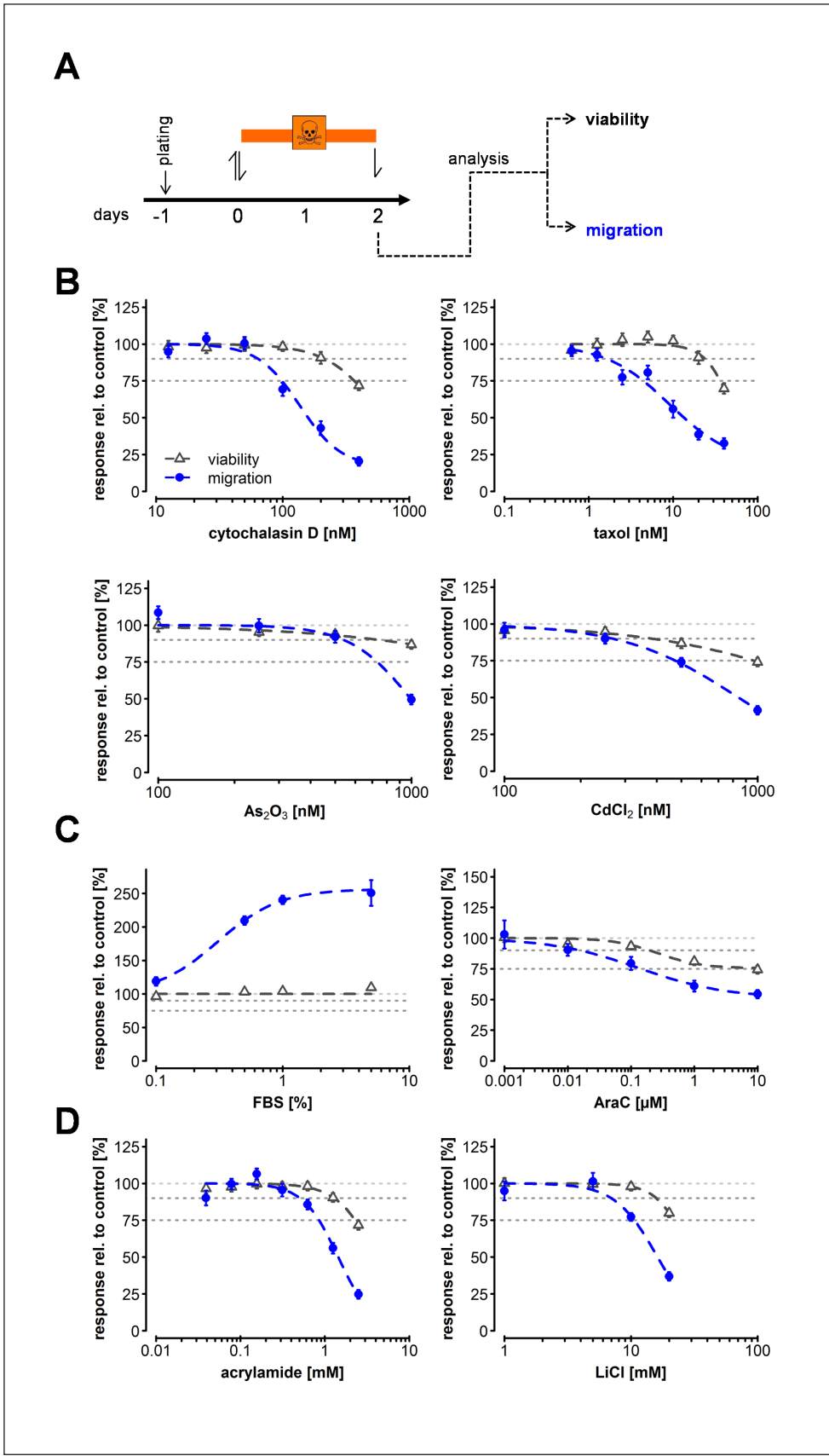


Fig. S3: Initial testing of assay performance under conditions used earlier for MINC scratch assays (48 h exposure)

(A) A graphical representation of the assay procedure informs on the exposure scheme and test endpoints: cells (plated at 30,000/well) were treated for 48 h with compounds, followed by measurements of viability and migration at the end of the exposure period. Concentration-response curves were obtained for selected compounds, and all values were normalized to untreated controls. (B) Examples for positive control compounds; (C) Endpoint-specific controls for increased migration (FBS) and for the role of cell proliferation in the assay (mitotic inhibitor: AraC); (D) Exemplary test compounds from the class of environmental toxicants (acrylamide) and drugs (LiCl). The light gray dotted line indicates the 100% y-axis value for easier reading of the diagrams. The other two dotted lines are drawn at 90% (indicating threshold for reduced viability) and at 75% (indicating threshold for reduced migration). Data are means ± SD from three different experiments. Statistical evaluations were not performed; data are intended for visual overview.

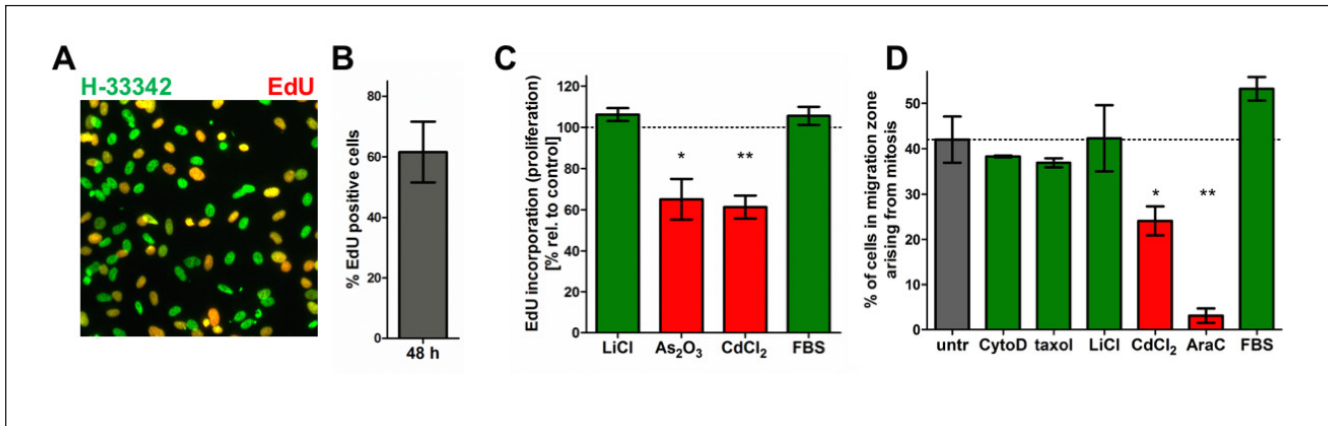


Fig. S4: Characterization of cell proliferation under conditions used earlier for MINC scratch assays (48 h exposure)

Cells were seeded as in Fig. 2 under standard cMINC assay conditions, and incubated for 48 h with 10 μ M EdU. Then, cells were stained for EdU incorporated into the DNA of proliferating cells (red), and co-stained with H-33342 (green). (A) In a representative picture double-positive cells are seen as yellow/orange. (B) The fraction of cells that had replicated their DNA within 48 h (EdU incorporation) was quantified by counting (means \pm SD, $n = 8$). (C) Cells were treated with LiCl (10 mM), As_2O_3 (1 μ M), $CdCl_2$ (1 μ M) or fetal bovine serum (FBS, 1%) for 48 h and EdU incorporation was assessed. Data were normalized to untreated control cells; (D) A migration experiment (as described in Suppl. Fig. S3A) was performed, and cells in the migration zone were imaged every 10 minutes using time-lapse video microscopy. The number of cells arising from mitosis in the circular region of interest (ROI) was determined from evaluation of the video tracks. For control cells, 185 ± 17 mitoses occurred. This number was normalized to the number of cells in the ROI at the end of the assay. Under control conditions, 442 ± 35 cells migrated into the ROI (e.g., $42.7\% \pm 5.1\%$ of cells in the ROI were generated by proliferation instead of migration from the outside); * $p < 0.05$; ** $p < 0.01$ (conditions with inhibited proliferation are highlighted in red).

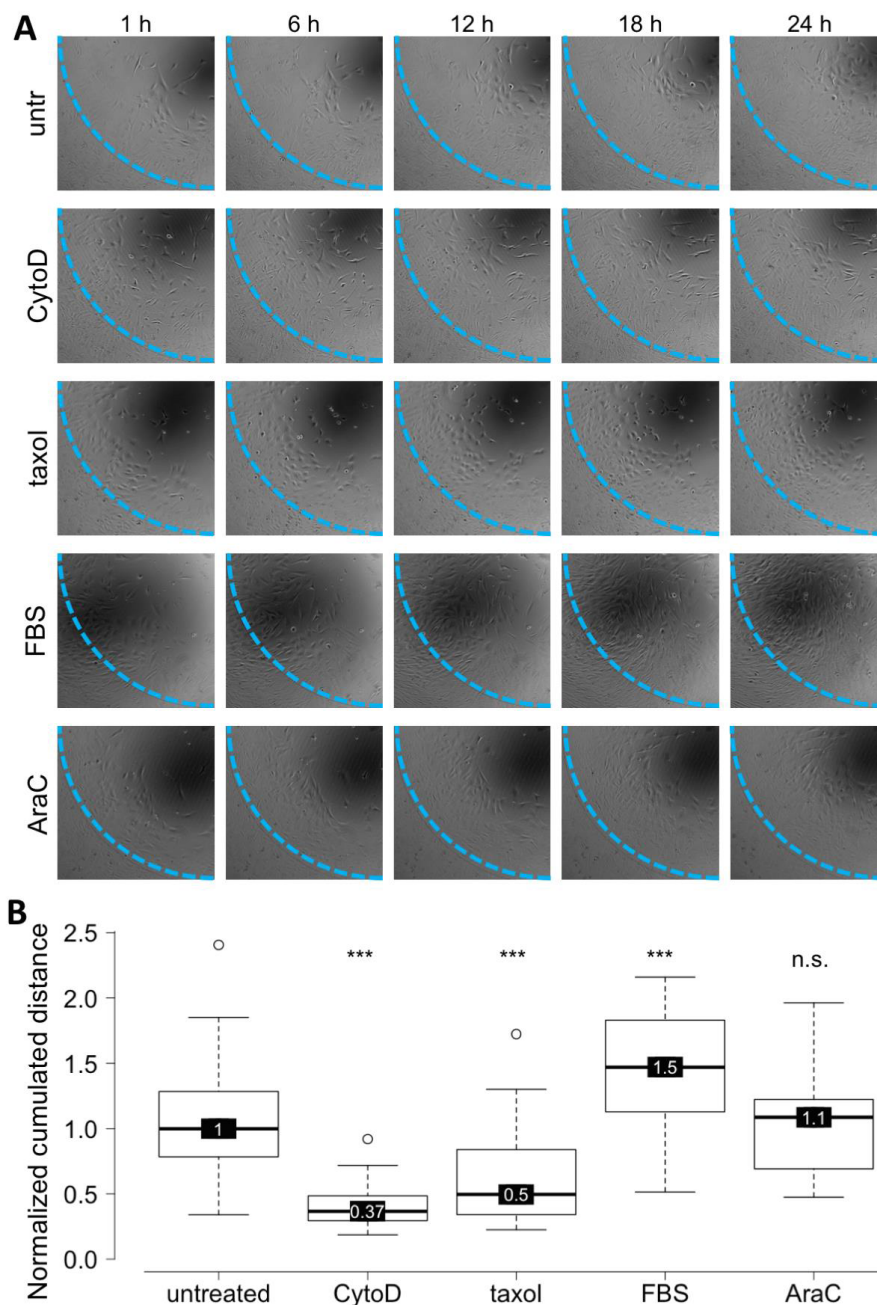


Fig. S5: Time-lapse video microscopy for cell tracking in the new cMINC assay format

NCCs were thawed and plated at 30,000/well. After one day, silicone stoppers were removed and medium was changed. Another 24 h later, treatment with CytoD (200 nM), taxol (10 nM), FBS (4%) and AraC (1 μ M) was initiated. Cell behavior was recorded for 24 h by phase contrast time-lapse video microscopy. (A) Representative still images from the video sequence are shown for selected time points. The width of one micrograph corresponds to 1 mm. The dashed line indicates the approximate position of the migration zone. Note that only the lower left quarter of the total image (and migration zone) is shown. (B) For each treatment condition, ten individual cells were traced, and for each control about 20-30 cells were traced. For each cell, the total distance of movement along its migration track was measured. All data were normalized to untreated controls in the same experiment. As the box-and-whisker plot displays data of three different experiments, each box represents the results of 30 (treatment) or 80 (controls) tracked cells. The box represents the first and third quartiles, the black line the median (number given in the black square) and the whiskers are at an interquartile range of 1.5. CytoD, cytochalasin D; FBS, fetal bovine serum; AraC, cytosine arabinoside; *** $p < 0.001$, n.s.: not significant.

**Supporting information references**

- Chambers, S. M., Mica, Y., Lee, G. et al. (2016). Dual-SMAD inhibition/WNT activation-based methods to induce neural crest and derivatives from human pluripotent stem cells. *Methods Mol Biol* 1307, 329-343. https://doi.org/10.1007/7651_2013_59
- Choi, I. Y., Lim, H. and Lee, G. (2014). Efficient generation human induced pluripotent stem cells from human somatic cells with Sendai-virus. *J Vis Exp* 86, e51406. <https://doi.org/10.3791/51406>
- Mica, Y., Lee, G., Chambers, S. M. et al. (2013). Modeling neural crest induction, melanocyte specification, and disease-related pigmentation defects in hESCs and patient-specific iPSCs. *Cell Rep* 3, 1140-1152. <https://doi.org/10.1016/j.celrep.2013.03.025>
- Schindelin, J., Arganda-Carreras, I., Frise, E. et al. (2012). Fiji: An open-source platform for biological-image analysis. *Nat Methods* 9, 676-682. <https://doi.org/10.1038/nmeth.2019>